Electronic Supplementary Material (ESI) for Inorganic Chemistry Frontiers.

Electronic Supplementary Information

Mechanism of action of an Ir(III) Complex Bearing a Boronic Acid Active as H_2O_2-Responsive Photosensitizer: ROS Generation and Quinone Release for GSH Scavenging

*Pierraffaele Barretta, Gloria Mazzone**

Department of Chemistry and Chemical Technologies, University of Calabria, 87036 Rende (CS), Italy.

Table of Contents

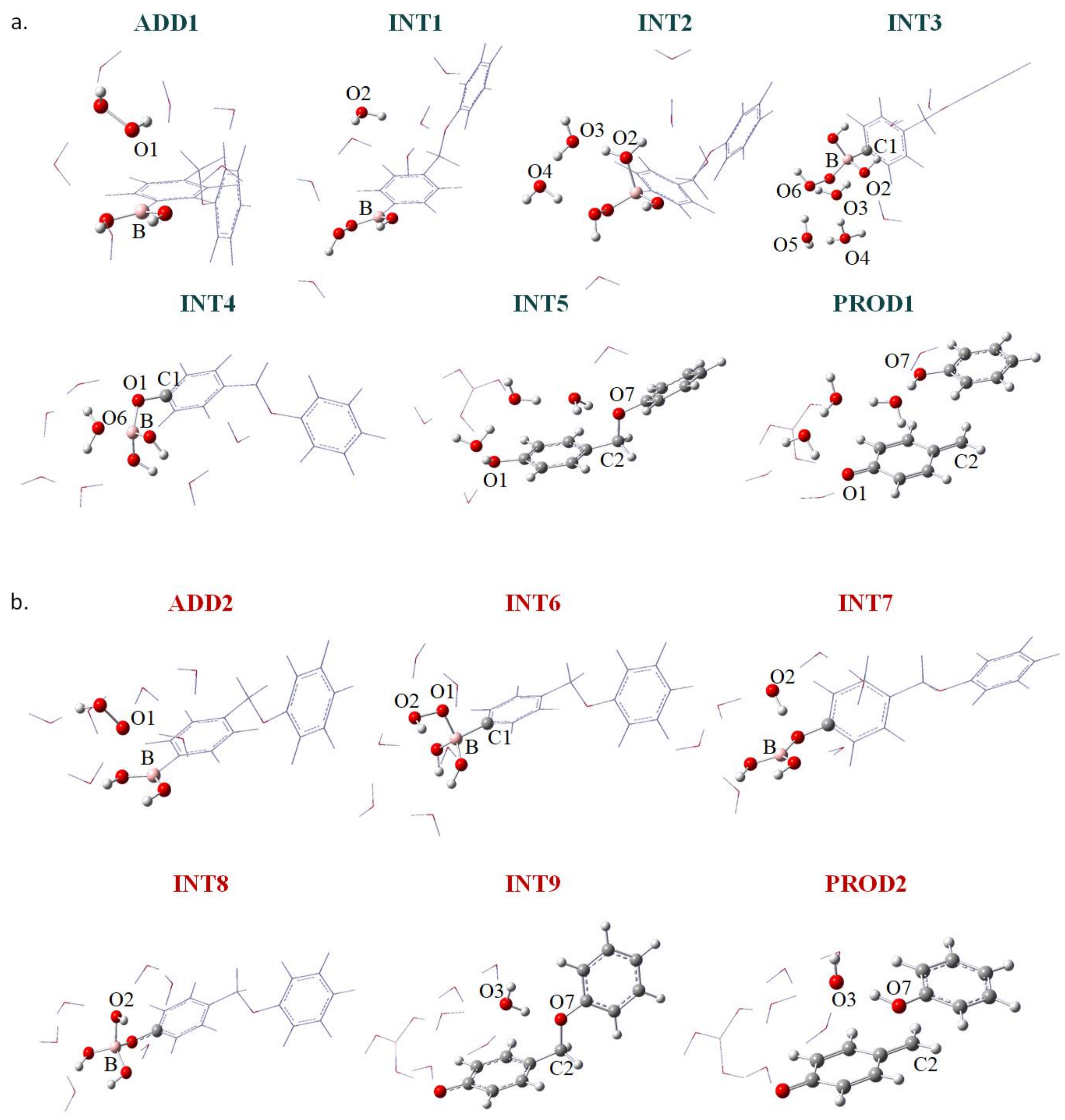

Figure S1. Optimized structures of the minima intercepted along both a) neutral and b) anion pathways.

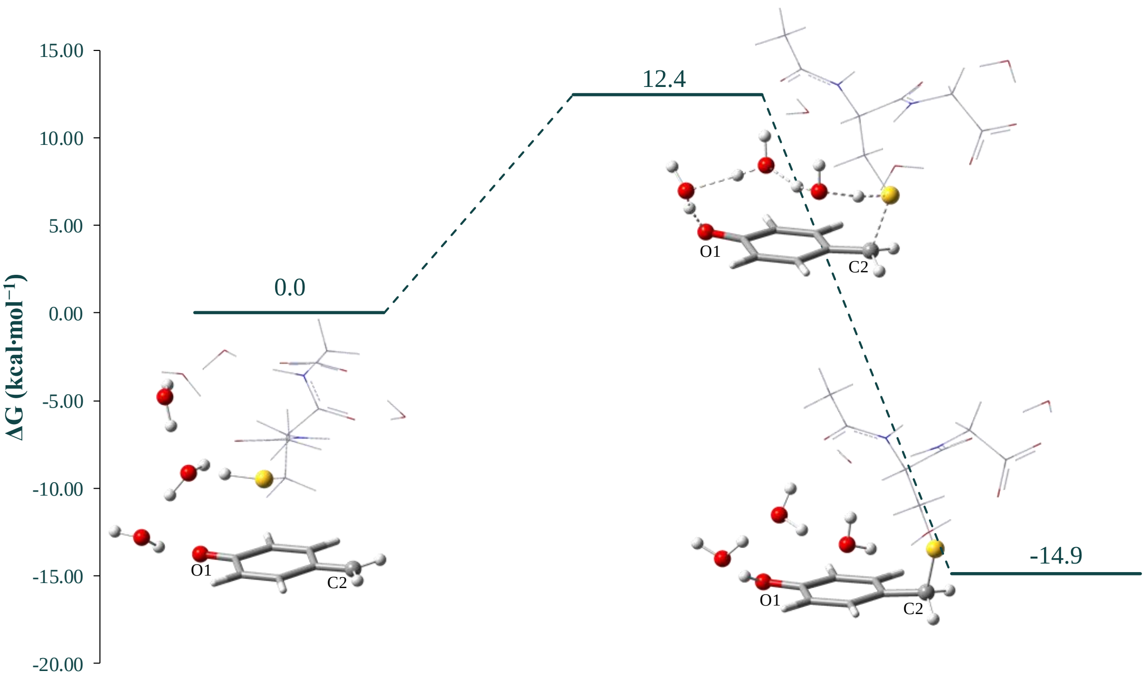

Figure S2. Free energy profiles in water describing the GSH alkylation by QM computed at B3LYP/6-31G(d,p) level of theory. The optimized structures of adduct, TS and product are included.

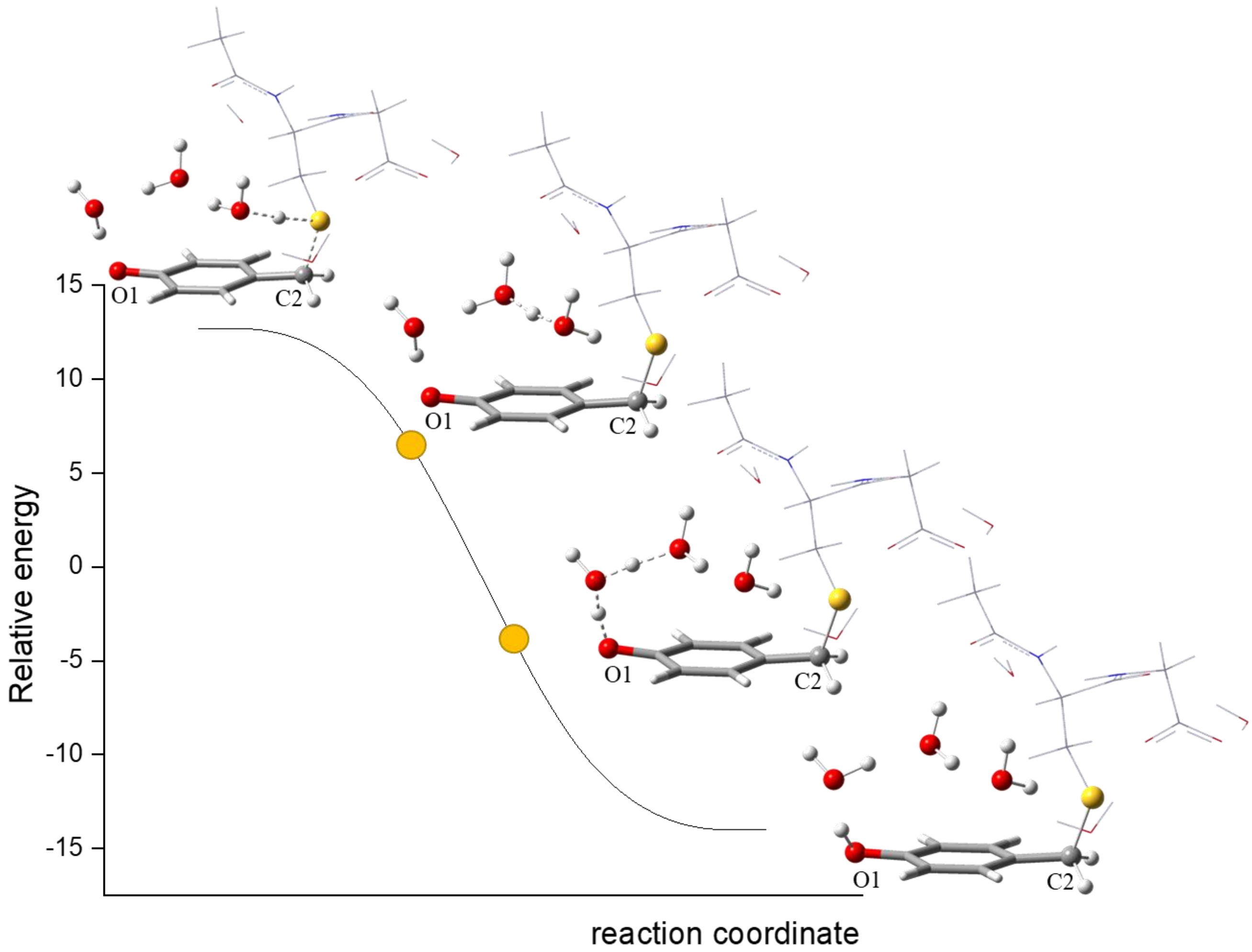

Figure S3. Intrinsic reaction coordinate calculation of TS’’ in the forward direction leading to product formation.

Table S1. Benchmark of exchange and correlation functional on the maximum absorption wavelength in water, λ_{max} in nm, for **Ir-OH** employing the 6-311G(d) basis set for C, N, H, O and the pseudopotential with its split-valence basis set SDD for Ir atom. Oscillator strength (*f*) is also reported.

	λ_{max} (nm)	*f*	Δ
Exp	*405*		
B97D	599.3	0.011	194.3
PBE	608.4	0.012	203.4
B3LYP	462.3	0.023	57.3
B3PW91	461.0	0.023	56.0
PBE0	433.0	0.030	28.0
M06L	554.6	0.013	149.6
CAM-B3LYP	351.7	0.161	-53.3
WB97XD	347.3	0.159	-57.7
LC-WHPBE	312.4	0.315	-92.6
M06	450.8	0.023	45.8
M11	315.6	0.329	-89.4
MN15	382.5	0.070	-22.5
MN15L	497.2	0.017	92.2
MN12L	502.0	0.022	97.0
N12	612.1	0.011	207.1
TPSS	576.0	0.014	171.0
M08HX	341.8	0.220	-63.2

Table S2. Benchmark of exchange and correlation functional on the maximum absorption wavelength in water, λ_{max} in nm, for **Ir-OH** employing the 6-311G(d,p) basis set for C, N, H, O and the pseudopotential with its split-valence basis set SDD for Ir atom. Oscillator strength (*f*) is also reported.

	λ_{max} (nm)	*f*	Δ
6-311G(d,p)	433.0	0.030	28.0
6-311+G(d,p)	434.2	0.029	29.2
6-311++G(d,p)	434.2	0.029	29.2
6-311++G(3df,2pd)	436.3	0.029	31.3

Discussion on benchmark

The exchange and correlation functionals used for reproducing the maximum absorption wavelength of **Ir-OH** complex are of different type: the GGA (general gradient approximation) functionals B97D[1], and PBE[2,3], the metaNGA (nonseparable gradient approximations) MN15[4] and N12[5], the meta-GGA M06L[6], MN15L[7] and MN12L[8], the global-hybrid GGA B3LYP[9,10], PBE0[11], M08-HX[12] and B3PW91[13], the global-hybrid meta-GGA M06[14], M11[15] and TPSS[16] and the range-separated hybrid GGA LC-WHPBE[17], CAM-B3LYP[18] and ωB97XD[19]. From data reported in Table S1 it can be inferred that some functionals strongly failed in reproducing the λ_{max}, see for instance N12 or B97D. While hybrid functionals like B3LYP and B3PW91 essentially give the same results, overestimating the λ_{max} by approximately 50 nm, PBE0 is one of the functional that better simulate such property. The range separated functionals underestimate it by about 50 nm, again the exception is for a functional belonging to the PBE family, that is the LC-wHPBE that fails in reproducing. Even the Minnesota functionals return very diversified results; while the metaNGA MN15 reproduces the λ_{max} with an error of 22.5 nm, a severe overestimation (M06, M06L, MN15L, MN12L, N12) or underestimation (M11) has been found employing the others. However, the result of the benchmark study returns the hybrid functionals MN15 and PBE0 as the most suitable in reproducing one of the main properties for PDT application. In particular, while MN15 underestimates of 22 nm the recorded wavelength, PBE0 reproduces the λ_{max} with an error of 28 nm.

Hence, once fixed the exchange and correlation functional, the influence of the basis set size has been checked as well. In particular, one and two diffuse functions have been added first, and then d-type functions has been added to the basis set with valence p orbitals, and f-functions to the basis set with d-type orbitals (Table S2). However, the outcomes confirm that 6-311G** basis set is enough accurate in reproducing the maximum experimental absorption wavelength of 405 nm, as with the other basis sets a slight red-shift of the lambda has been observed.

Table S3. Excitation energies (ΔE, eV), absorption wavelength (λ, nm), oscillator strength (f), MO contribution (%) for Ir(III) complexes, **Ir-B(OH)$_2$** and **Ir-OH**.

Complex	ΔE	λ	*f*[a]	MO contribution	Theoretical Assignment	λ^{exp}
Ir-B(OH)$_2$	2.86	433	0.032	H → L 85%	ML$_1$CT/LL$_1$CT	405[b]
	3.55	350	0.181	H-3 → L 39%; H-4 → L 15%; H-1 → L+1 15%	LL$_1$CT/ML$_1$CT	
	4.08	304	0.383	H-1 → L+4 29%; H-1 → L+3 26%	L$_1$LCT/IL$_1$CT	
	4.11	302	0.315	H-1 → L+4 39%; H-1 → L+3 23%	L$_1$LCT/IL$_1$CT	
	4.20	296	0.152	H → L+5 18%; H-3 → L+2 11%; H-1 → L+2 10%; H-1 → L+4 10%	MLCT/IL$_1$CT	
	4.34	286	0.105	H-9 → L 31%; H-5 → L+1 27%	ML$_1$CT/IL$_1$CT	
	4.50	275	0.166	H-5 → L+2 46%; H-2 → L+5 12%	MLCT/ILCT	
	4.52	274	0.136	H-13 → L 32%; H-11 → L 13%; H-5 → L+2 10%	ML$_1$CT/LL$_1$CT	
	4.62	268	0.542	H-9 → L+1 35%; H-6 → L+1 13%	IL$_1$CT/ML$_1$CT	
	4.73	262	0.171	H-3 → L+4 11%; H-12 → L 10%	ML$_1$CT/LL$_1$CT	
Ir-OH	2.86	433	0.030	H → L 89%	ML$_1$CT/LL$_1$CT	405[b]
	3.55	349	0.170	H-3 → L 30%; H-1 → L+1 29%; H-4 → L 11%	ML$_1$CT/LL$_1$CT	
	4.10	303	0.112	H-1 → L+3 42%; H-2 → L+3 10%	MLCT/L$_1$LCT	
	4.13	300	0.310	H-1 → L+4 53%; H → L+5 11%	ML$_1$CT/IL$_1$CT	
	4.21	295	0.188	H → L+5 17%, H-3 → L+2 12%; H-1 → L+2 12%; H-1 → L+4 12%	ML$_1$CT/LL$_1$CT	
	4.35	285	0.109	H-7 → L 33%; H-5 → L+1 20%	ML$_1$CT/IL$_1$CT	
	4.50	275	0.157	H-5 → L+2 45%; H-2 → L+5 12%	ILCT/LMCT	
	4.52	274	0.110	H-11 → L 32%; H-9 → L 15%; H-12 → L 10%	LL$_1$CT/ML$_1$CT	
	4.65	267	0.457	H-7 → L+1 43%; H-11 → L 10%; H-10 → L 10%	IL$_1$CT/ML$_1$CT	
	4.74	261	0.157	H-6 → L+1 18%; H-7 → L+1 13%; H-1 → L+6 13%	IL$_1$CT/ML$_1$CT	

a. Only vertical transition with *f* greater than 0.1 are reported, with the exception of the most red-shifted transition. b. from [20].

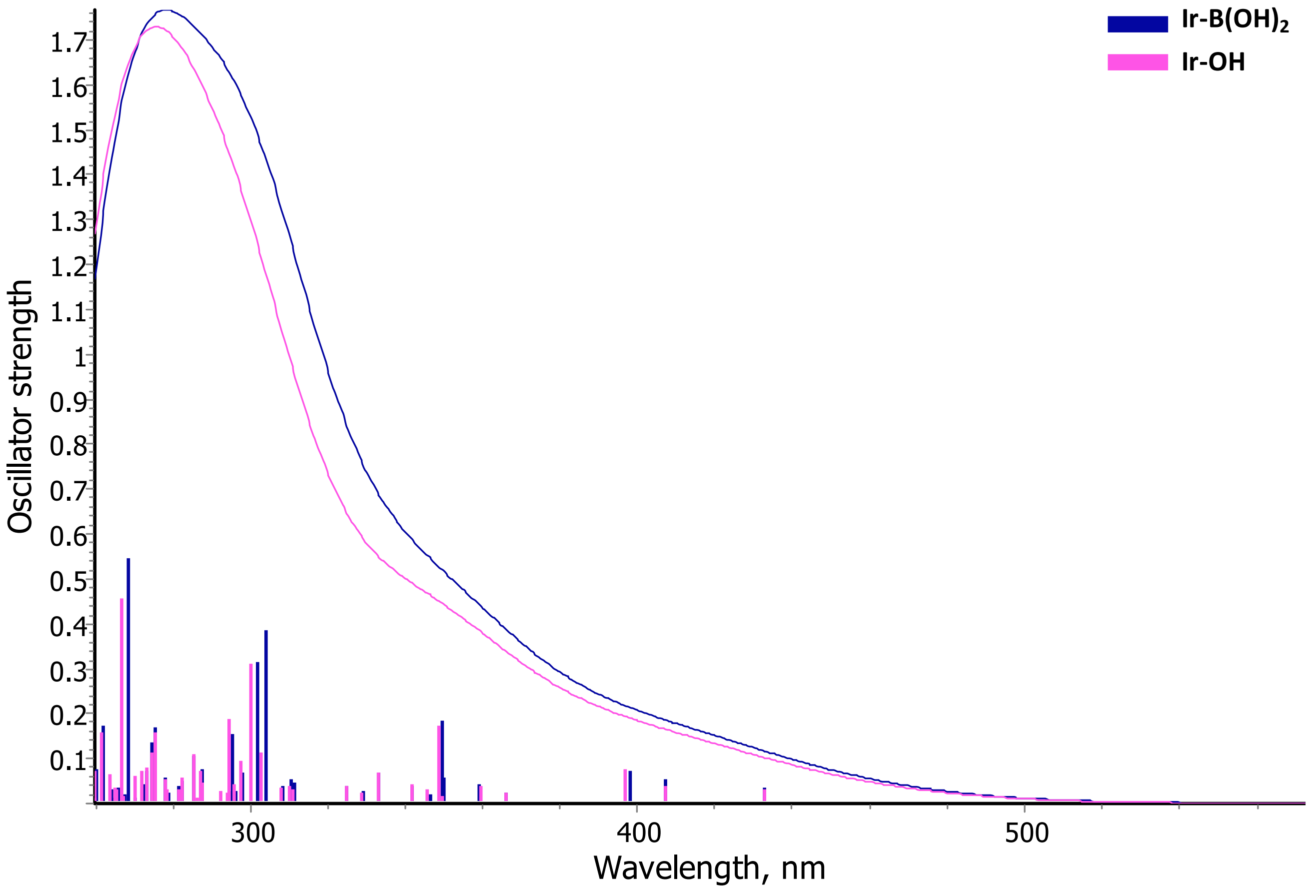

Figure S4. Computed UV–Vis spectra of the studied species, in water, at the PBE0/6-311G(d,p)/SDD level of theory. The convolution of the spectra was accomplished with a half-width of 0.27 eV.

Table S4. Lowest triplet states excitation energies (ΔE, eV), MO contribution (%) and Theoretical Assignment for the investigated Ir(III) complexes.

Complex	State	ΔE	MO contribution	Theoretical Assignment
Ir-B(OH)$_2$	T1	2.59	H-1 → L+1 26%; H → L 18%; H → L+1 17%	IL$_1$CT/MC
	T2	2.63	H → L 43%; H-1 → L 29%	IL$_1$CT/MC
	T3	2.77	H → L+2 35%; H-1 → L+2 11%; H-4 → L+2 10%	ILCT/MC
	T4	2.83	H-1 → L 44%; H → L 23%	LL$_1$CT/MC
	T5	2.84	H-2 → L+3 28%; H-3 → L+3 15%	ILCT/MC
Ir-OH	T1	2.59	H-1 → L+1 29%; H → L 19%; H → L+1 13%	IL$_1$CT/MC
	T2	2.63	H → L 38%; H-1 → L 35%	IL$_1$CT/MC
	T3	2.77	H → L+2 40%; H-4 → L+2 11%	ILCT/MC
	T4	2.83	H-1 → L 39%; H → L 27%	LL$_1$CT/MC
	T5	2.84	H-2 → L+3 25%; H-3 → L+3 14%	ILCT/MC

	hole	*particle*	*character*
S_1	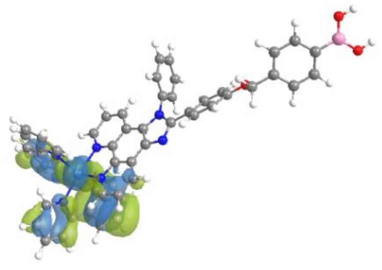	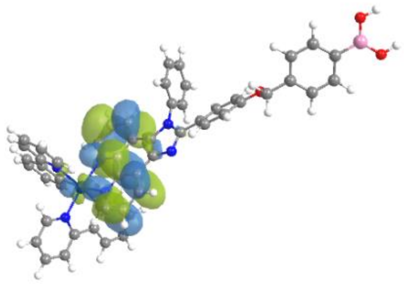	LL_1CT/ML_1CT
T_1	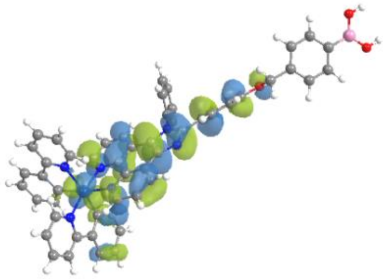	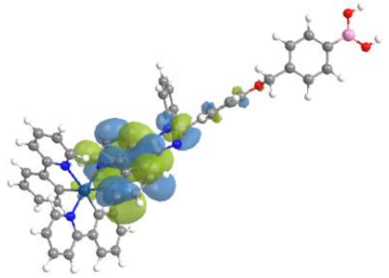	IL_1CT/MC
T_2	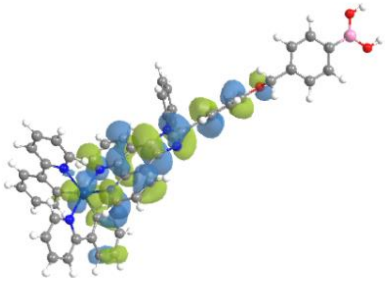	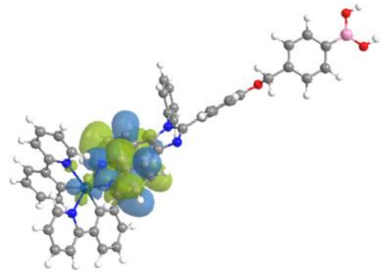	IL_1CT/MC
T_3	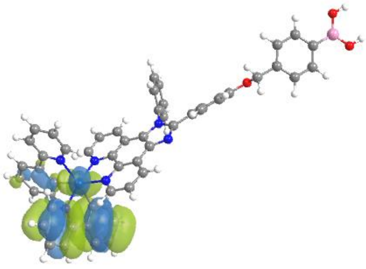	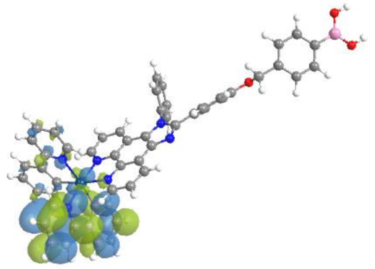	ILCT/MC
T_4	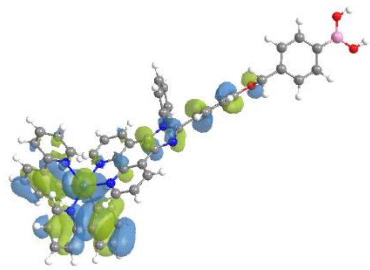	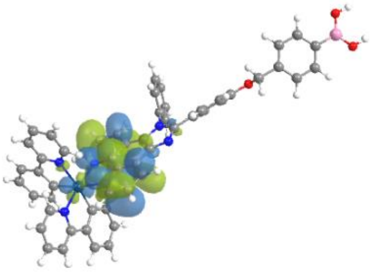	LL_1CT/MC
T_5	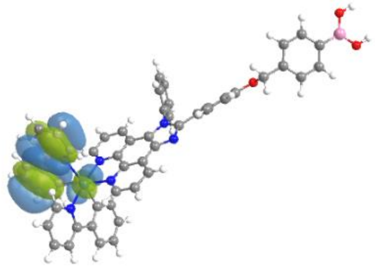	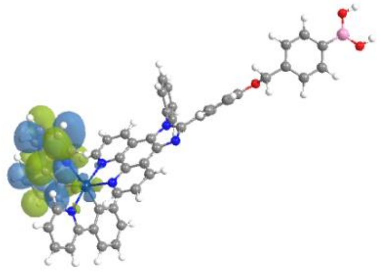	ILCT/MC

Figure S5. NTOs of the bright and triplet states computed for **Ir-B(OH)$_2$**.

References

1 S. Grimme, Semiempirical GGA-type density functional constructed with a long-range dispersion correction, *J. Comput. Chem.*, 2006, **27**, 1787–1799.

2 J. P. Perdew, K. Burke and M. Ernzerhof, Generalized Gradient Approximation Made Simple, *Phys. Rev. Lett.*, 1996, **77**, 3865.

3 J. P. Perdew, K. Burke and M. Ernzerhof, Generalized Gradient Approximation Made Simple [Phys. Rev. Lett. 77, 3865 (1996)], *Phys. Rev. Lett.*, 1997, **78**, 1396.

4 H. S. Yu, X. He, S. L. Li and D. G. Truhlar, MN15: A Kohn–Sham global-hybrid exchange–correlation density functional with broad accuracy for multi-reference and single-reference systems and noncovalent interactions, *Chem. Sci.*, 2016, **7**, 5032.

5 R. Peverati and D. G. Truhlar, Exchange-correlation functional with good accuracy for both structural and energetic properties while depending only on the density and its gradient, *J. Chem. Theory Comput.*, 2012, **8**, 2310–2319.

6 Y. Zhao and D. G. Truhlar, A new local density functional for main-group thermochemistry, transition metal bonding, thermochemical kinetics, and noncovalent interactions, *J. Chem. Phys.*, 2006, **125**, 194101.

7 H. S. Yu, X. He and D. G. Truhlar, MN15-L: A New Local Exchange-Correlation Functional for Kohn-Sham Density Functional Theory with Broad Accuracy for Atoms, Molecules, and Solids, *J. Chem. Theory Comput.*, 2016, **12**, 1280–1293.

8 R. Peverati and D. G. Truhlar, An improved and broadly accurate local approximation to the exchange–correlation density functional: The MN12-L functional for electronic structure calculations in chemistry and physics, *Phys. Chem. Chem. Phys.*, 2012, **14**, 13171–13174.

9 A. D. Becke, Density-functional thermochemistry. III. The role of exact exchange, *J. Chem. Phys.*, 1998, **98**, 5648.

10 C. Lee, W. Yang and R. G. Parr, Development of the Colle-Salvetti correlation-energy formula into a functional of the electron density, *Phys. Rev. B*, 1988, **37**, 785.

11 C. Adamo and V. Barone, Toward reliable density functional methods without adjustable parameters: The PBE0 model, *J. Chem. Phys.*, 1999, **110**, 6158.

12 Y. Zhao and D. G. Truhlar, Exploring the limit of accuracy of the global hybrid meta density functional for main-group thermochemistry, kinetics, and noncovalent interactions, *J. Chem. Theory Comput.*, 2008, **4**, 1849–1868.

13 J. P. Perdew and K. Burke, Generalized gradient approximation for the exchange-correlation hole of a many-electron system, *Phys. Rev. B*, 1996, **54**, 16533.

14 Y. Zhao and D. G. Truhlar, The M06 suite of density functionals for main group thermochemistry, thermochemical kinetics, noncovalent interactions, excited states, and transition elements: two new functionals and systematic testing of four M06-class functionals and 12 other function, *Theor. Chem. Acc.*, 2008, **120**, 215–241.

15 R. Peverati and D. G. Truhlar, Improving the accuracy of hybrid meta-GGA density functionals by range separation, *J. Phys. Chem. Lett.*, 2011, **2**, 2810–2817.

16 J. Tao, J. P. Perdew, V. N. Staroverov and G. E. Scuseria, Climbing the density functional ladder: Nonempirical meta–generalized gradient approximation designed for molecules and solids, *Phys. Rev. Lett.*, 2003, **91**, 146401.

17 O. A. Vydrov and G. E. Scuseria, Assessment of a long-range corrected hybrid functional, *J. Chem. Phys.*, 2006, **125**, 234109.

18 T. Yanai, D. P. Tew and N. C. Handy, A new hybrid exchange–correlation functional using the Coulomb-attenuating method (CAM-B3LYP), *Chem. Phys. Lett.*, 2004, **393**, 51–57.

19 J. Da Chai and M. Head-Gordon, Long-range corrected hybrid density functionals with damped atom–atom

dispersion corrections, *Phys. Chem. Chem. Phys.*, 2008, **10**, 6615–6620.

20 X. Liao, J. Shen, W. Wu, S. Kuang, M. Lin, J. Karges, Z. Tang and H. Chao, A mitochondrial-targeting iridium(iii) complex for H2O2-responsive and oxidative stress amplified two-photon photodynamic therapy, *Inorg. Chem. Front.*, 2021, **8**, 5045–5053.